

3D-Pix: 3D Editing with Single-Shot Multi-View Diffusion and Gaussian Splatting

Anonymous CVPR submission

Paper ID 22

Abstract

001 *The rapid advancements in 3D visual generative AI are*
 002 *driven by improvements in the quality and realism of 2D*
 003 *generative models, alongside recent developments in effi-*
 004 *cient 3D reconstruction techniques. In this work, we ad-*
 005 *dress the problem of 3D editing by developing a consistent*
 006 *multi-view 2D editing model and leveraging 3D reconstruc-*
 007 *tion methods to obtain a 3D representation. Our approach*
 008 *generalizes across various inputs, including renderings of*
 009 *digital 3D assets and turntable videos of real-world objects.*
 010 *Furthermore, this generalization enables our method to be*
 011 *applied as a post-processing step to any existing 3D gener-*
 012 *ative approach, regardless of the underlying geometry rep-*
 013 *resentation model.*

014 *We introduce 3D-Pix, a model that integrates 2D genera-*
 015 *tion with 3D reconstruction to facilitate 3D editing. A key*
 016 *component of our approach is MV Instruct Pix2Pix XL, a*
 017 *modified version of Instruct Pix2Pix [4], designed to gen-*
 018 *erate consistent multi-view images of the same object using*
 019 *the Stable Diffusion XL [37] image generation model. To*
 020 *ensure coherence across multiple views, we employ a novel*
 021 *interpolation mechanism that enables single-inference pro-*
 022 *cessing for consistent editing across multiple images. Ad-*
 023 *ditionally, we enhance output fidelity by incorporating a*
 024 *super-resolution upscaling step. The geometry of the asset*
 025 *is estimated using a state-of-the-art 3D Gaussian Splatting*
 026 *[22] model. Our proposed 3D-Pix model effectively bal-*
 027 *ances appearance refinement and geometric accuracy, par-*
 028 *ticularly in preserving high-frequency details and achieving*
 029 *high-fidelity results.*

030 1. Introduction

031 The field of 3D visual generative AI is undergoing signifi-
 032 cant growth, driven by advances in the quality and realism
 033 of 2D generative models, as well as breakthroughs in novel
 034 3D reconstruction techniques, such as 3D Gaussian Splat-
 035 ting [22]. The increasing demand for automation in the

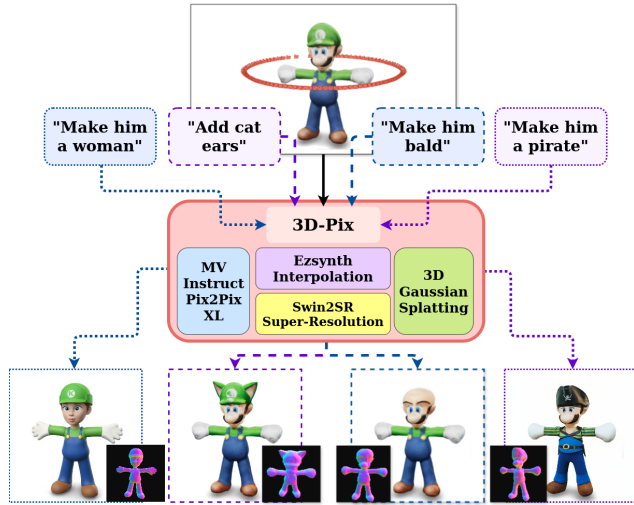


Figure 1. Our 3D-Pix editing high-level process. We expect a turn-around sequence and the edit prompt on input, and our 3D-Pix returns the edited and reconstructed 3D model.

036 creation of high-quality 3D assets has further accelerated
 037 research in this domain.

038 The 3D generative domain comprises various tasks,
 039 commonly classified with respect to input modalities: text-
 040 to-3D [8, 32, 38, 43, 43, 47, 58, 70, 71], image-to-3D
 041 [12, 27, 29, 49, 50, 61, 72], and 3D-to-3D or editing genera-
 042 tions [1, 4, 15, 18, 34, 35]. Although many approaches exist
 043 in each direction, many use outdated 2D generative and 3D
 044 reconstruction approaches, providing low resolution of the
 045 estimated 3D model. Moreover, the 3D-to-3D direction is
 046 often treated as re-texturing, aiming to modify only the ap-
 047 pearance with no geometry changes.

048 In this work, we introduce an advanced implicit 3D edit-
 049 ing algorithm that operates solely on text prompts, eliminat-
 050 ing the need for explicit manual masks or bounding boxes to
 051 specify the target region for editing. Our approach presents
 052 a novel 3D editing pipeline that integrates sequential com-
 053 ponents of 3D reconstruction using 3D Gaussian Splatting
 054 [22] with a multi-view editing framework. This framework

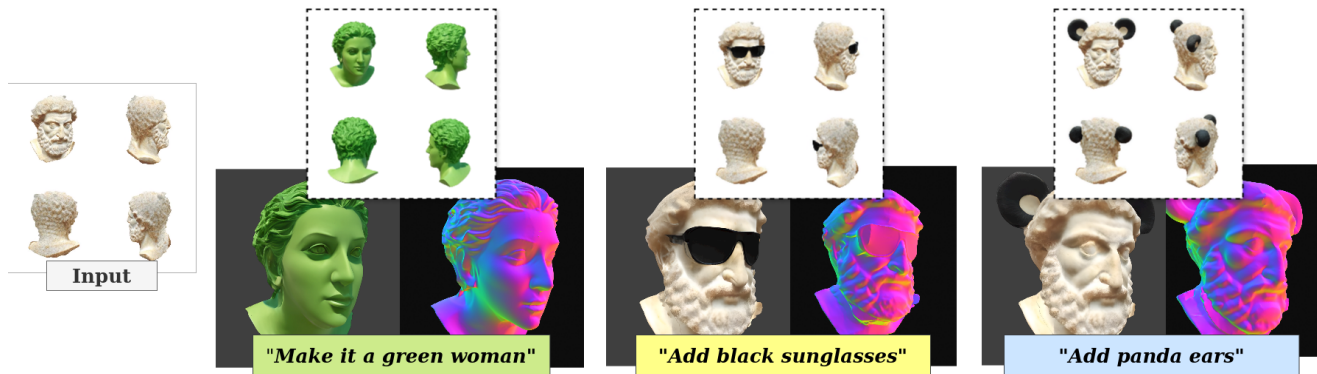


Figure 2. Our 3D-Pix text-guided edit renderings of the reconstructed 3D models.

055 leverages the Stable Diffusion XL [37] generative model
056 and the 2D editing capabilities of Instruct Pix2Pix [4], al-
057 lowing high-fidelity text-guided modifications of 3D assets.

058 In summary, our contributions are:

- 059 • We propose a novel Multi-View Instruct Pix2Pix XL
060 model, a modified version of the original 2D editing
061 model Instruct Pix2Pix [4] to generate consistent multi-
062 view frames of the same object using the SOTA Stable
063 Diffusion XL [37] generative model.
- 064 • We propose our 3D editing model 3D-Pix by leveraging
065 our pre-trained Multi-View Instruct Pix2Pix XL model in
066 a single-inference manner due to being coupled with the
067 complex interpolation logic, together with the 3D Gaus-
068 sian Splatting [22] geometry reconstruction.
- 069 • We demonstrate the generalization of 3D-Pix to various
070 real-life and digital inputs and its application as a post
071 hoc stage for an arbitrary 3D generative model of any ge-
072 ometry representation technique.

073 2. Related Works

074 2.1. Diffusion Models

075 Although diffusion generative models were first introduced
076 by Sohl-Dickstein *et al.* [45], they gained widespread at-
077 tention following the DDPM work [20], which signifi-
078 cantly improved diffusion processes and sampling strate-
079 gies. DDIM [46] further enhanced efficiency by introducing
080 a non-Markovian denoising process, enabling faster sam-
081 pling with superior quality.

082 Although diffusion models eventually surpassed GANs
083 in quality [14], they remained computationally expensive
084 due to their high-dimensional pixel-space operations. The
085 Latent Diffusion Model (LDM) [39] addressed this by in-
086 corporating a VAE, reducing dimensionality and improving
087 efficiency.

088 Stable Diffusion (SD) [39] became the most widely
089 adopted LDM implementation. Despite numerous advance-
090 ments [21, 33, 60, 69, 77], the most recognized diffusion

091 model today is Stable Diffusion XL [37], which achieves
092 state-of-the-art realism and quality.

093 2.2. 3D Representation Models

094 When estimating a 3D model from a set of images, geo-
095 metry can be represented using explicit or implicit techniques.
096 Explicit representations are widely used due to their sim-
097 plicity and efficiency, with common approaches including
098 3D voxels [9, 41, 67], meshes [16, 17, 36, 56], and point
099 clouds [26, 48, 63, 73].

100 Implicit representations are also widely adopted, with
101 many works leveraging signed distance functions (SDF)
102 [7, 42, 44, 64] and occupancy fields [28, 74, 75]. How-
103 ever, NeRF [30] and its extensions [2, 6, 13, 29, 54, 55, 68]
104 dominate much of the research in implicit 3D modeling.

105 Despite extensive efforts to accelerate NeRF, even the
106 latest optimizations remain computationally demanding. A
107 significantly faster alternative is 3D Gaussian Splatting (3D
108 GS) [22], which not only surpasses NeRF in speed but also
109 achieves superior visual quality while enabling real-time
110 rendering. Due to its efficiency, 3D GS is increasingly being
111 adopted in 3D generation tasks [8, 23, 24, 31, 62, 65].

112 2.3. Text-to-3D

113 One of the most influential works in text-to-3D generation
114 using diffusion models is DreamFusion [38], which intro-
115 duced the Score Distillation Sampling (SDS) loss. This
116 novel loss function operates in parameter space, using a
117 frozen diffusion model as a critic to guide NeRF optimiza-
118 tion. SDS remains a fundamental component in many mod-
119 ern 3D generation methods [43, 47, 58, 70, 71].

120 A common strategy is training a multi-view diffusion, as
121 introduced in MVDream [43], to generate consistent multi-
122 views [51]. GSGEN [8] is among the first works to in-
123 tegrate 2D diffusion-based generation with 3D Gaussian
124 Splatting, coupled with pre-trained text-to-point-cloud dif-
125 fusion Point-E [32] and effective guidance of the geometry
126 estimation of 3D Gaussians using 3D SDS loss.

127 **2.4. Image-to-3D & Re-texturing**

128 The re-texturing problem differs from full 3D reconstruction
 129 as it often requires no geometry changes and can be addressed by generating PBR materials [25, 66]. However,
 130 these methods may not apply to implicit geometry, necessitating further optimization of the 3D model. Many image-
 131 to-3D models can also be adapted for re-texturing tasks [29, 72].

135 Latent-NeRF [29] was among the first diffusion-based
 136 methods to generate 3D objects using both text and image
 137 inputs, introducing a model for retexturing based on pattern images. IP-Dreamer [72] expanded this approach, being
 138 the first to implement Image Prompt (IP) control in Stable Diffusion with modifications to the SDS loss. Several
 139 other methods can generate 3D models from a single image
 140 [12, 27, 49, 61], with DreamGaussian [50] being the most
 141 relevant, as it utilizes 3D Gaussian Splatting for reconstruction.
 142

145 **2.5. 3D Editing**

146 The editing task gained significant popularity following
 147 the Prompt-to-Prompt work [19], which eliminated the
 148 need for manual mask selection and introduced edits con-
 149 trolled solely by text prompts through attention mech-
 150 anisms. This innovation has spurred further research in the
 151 domain [1, 4, 18, 35].

152 Recent approaches that leverage 3D Gaussian Splat-
 153 ting for geometry optimization include GSEdit [34], Gaus-
 154 sianEditor [15], View-consistent Editing (VcEdit) [57] and
 155 GaussCtrl [59] models. GSEdit [34] iteratively guides the
 156 reconstruction process using Score Distillation Sampling
 157 (SDS) loss with Instruct Pix2Pix as the diffusion model, al-
 158 lowing refined edits based on user prompts. GaussianEditor
 159 [15] separates editing tasks into object removal and incor-
 160 poration through semantic tracing, followed by Hierarchical
 161 Gaussian Splatting (HGS). VcEdit [57] introduces 3DGS
 162 coupled with Cross-attention and Editing Consistency mod-
 163 ules to improve multi-view consistency. GaussCtrl [59]
 164 employs depth guidance with ControlNet [76] to enhance
 165 geometric consistency and the attention-based latent code
 166 alignment module to improve texture consistency.

167 **3. Preliminary**168 **3.1. Instruct Pix2Pix**

169 Instruct Pix2Pix [4] is a state-of-the-art (SOTA) 2D diffu-
 170 sion model designed for text-guided image editing. The
 171 authors introduced a novel training methodology based on
 172 a synthetically generated dataset, leveraging Prompt-to-
 173 Prompt [19] and the GPT-3 language model [5] to create
 174 text-image editing pairs.

175 The dataset generation process consists of three key
 176 stages. First, an "edited prompt" is generated by condi-

177 tioning GPT-3 on the original image description and the
 178 given editing instruction, producing a modified description
 179 that aligns with the intended transformation. In the second
 180 stage, Stable Diffusion [39] and Prompt-to-Prompt [19] are
 181 employed to generate both the original and edited images
 182 corresponding to the prompts.

183 The model is trained by minimizing the latent diffusion
 184 objective function, conditioned on text input c_T and the im-
 185 age c_I :

$$L = \mathbb{E}_{\mathcal{E}(x), \mathcal{E}(c_I), c_T, \epsilon, t} \left[\|\epsilon - \epsilon_\theta(z_t, t, \mathcal{E}(c_I), c_T)\|_2^2 \right], \quad (1)$$

187 where z_t is the noisy latent variable after diffusing for t
 188 steps the input image x in a latent space with the encoder
 189 $z = \mathcal{E}(x)$.

190 **4. Approach**

191 Generation consistency for many images was proven to be
 192 a challenging task ([43]). Unlike GSEdit [34], which used
 193 Instruct Pix2Pix edits iteratively for geometry optimization
 194 with SDS loss, we edit the frames in only a single inference
 195 with our modified Instruct Pix2Pix model, making 2D edits
 196 and 3D reconstruction as independent processes.

197 The main idea of our approach is to process the edits
 198 described in the input prompt with a single inference of the
 199 generative model to achieve consistency. For that, we divide
 200 all of the input frames into specifically four orthogonal key
 201 frames and the rest of the intermediate (inter) frames. The
 202 key images capture the most information about the object
 203 from different angles, and the edits with the diffusion model
 204 are applied only to those with our proposed Multi-View
 205 variation of the Instruct Pix2Pix model [4] (see Sec. 4.2).
 206 The rest of the frames are edited by interpolating the edited
 207 key frames into the poses of the original inter frames (see
 208 Sec. 4.3) to achieve edits consistent with the key ones. The
 209 full pipeline is shown in Fig. 4. This idea is highly inspired
 210 by the 3D-GSR [3] work, which leverages consistent 3D
 211 Super-Resolution by leveraging 2D Super-Resolution and
 212 3D GS models.

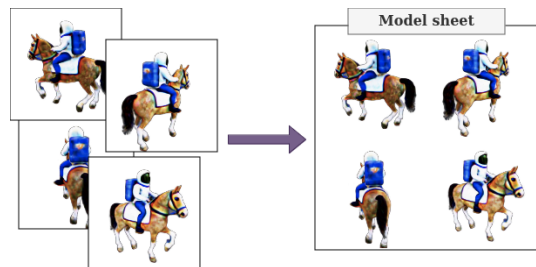


Figure 3. A model sheet is a single image composed as a grid of the orthogonal frames of the same object.

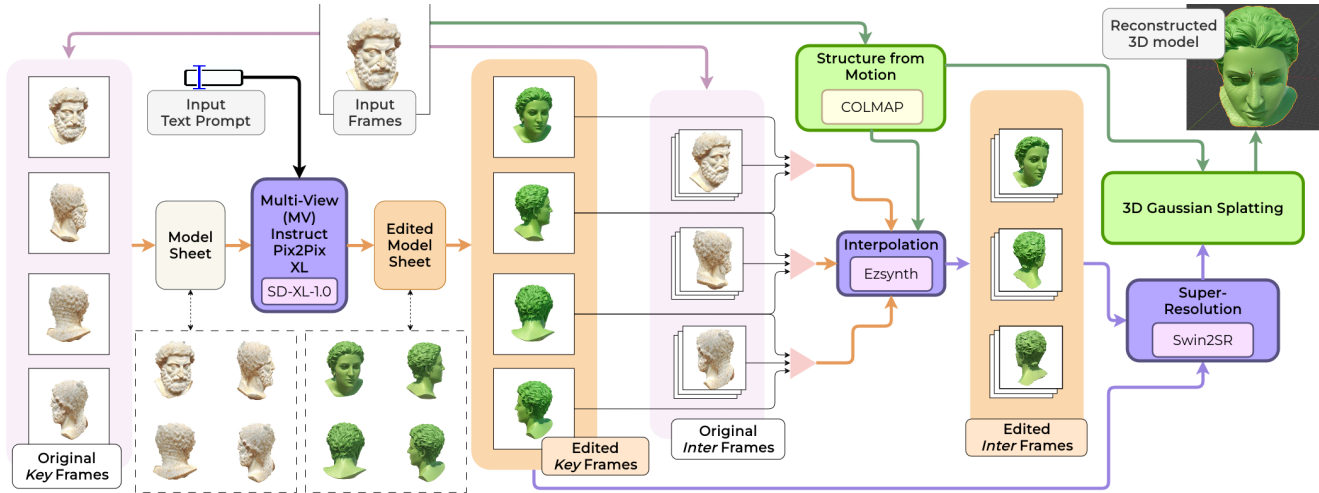


Figure 4. The complete architecture of 3D-Pix. Our proposed MV Instruct Pix2Pix XL is used to edit several key frames from the input sequence given the prompt guidance, and the complex interpolation algorithm is used to achieve the edits of all intermediate frames consistent with the already changed images. Once all of the frames are edited, the images are upscaled with a Super-Resolution model and passed to the 3D GS reconstruction together with the SfM point cloud created from the original sequence.

213

4.1. Model sheet

214
215
216
217
218
219

The idea is first introduced in MVDream [43] work, where the authors trained a multi-view diffusion model to generate four orthogonal views as a grid. Similar to their approach, we also compose a grid of orthogonal frames as in Fig. 3, which we call a model sheet, as the SD produces consistent generations when done in a single inference.

220

4.2. Multi-View Instruct Pix2Pix XL

221
222
223
224

Instruct Pix2Pix [4] is a high-fidelity, text-guided image editing model built upon the original Stable Diffusion v1 framework [39], capable of generating images at a resolution of 512×512 .

225
226
227
228
229
230
231
232
233
234
235

To enhance both the quality and resolution of 2D-generated outputs, we adapt the training methodology of Instruct Pix2Pix to a more advanced model—Stable Diffusion XL (SDXL) [37], which is approximately three times larger in scale. Specifically, we follow the modified training instructions provided in the official implementation (https://github.com/huggingface/diffusers/blob/main/examples/instruct_pix2pix/train_instruct_pix2pix_sdxl.py) and fine-tune the SDXL-base-1.0 checkpoint as our foundation.

236
237
238
239
240
241
242

Ensuring consistency in prompt-guided edits across multiple frames of a given sequence presents a key challenge. To address this, we employ a model sheet approach, wherein multiple key frames are aggregated into a single composite image (sheet). Edits are then applied in a single inference pass, preserving temporal and structural coherence across frames. To facilitate this, we modify the data

generation process for Instruct Pix2Pix while maintaining the original training pipeline, introducing Multi-View Instruct Pix2Pix XL (MV Instruct Pix2Pix XL) for multi-view editing.

For our dataset construction, we utilize Objaverse 1.0 [11], a large-scale collection of over 800K 3D models. To optimize computational resources—given the high cost of SDXL fine-tuning—we filter the dataset to include only high-definition (HD) models, reducing it to approximately 50K assets. From each selected 3D model, we generate random renderings from four orthogonal viewpoints, with an initial camera position randomly assigned. These renderings are then composed into model sheets, with each 3D asset yielding 10 different sheets from diverse perspectives, resulting in a total of 40 individual renders per object. Each model sheet is further paired with a unique editing prompt, ultimately producing 500K training samples.

Following the methodology outlined in the original Instruct Pix2Pix paper, we leverage the GPT-3 model [5] to generate triplets of text prompts. Each triplet consists of (1) an image caption, (2) an edit instruction, and (3) a caption describing the modified image. These structured prompts are then used in conjunction with Stable Diffusion and Prompt-to-Prompt [19] to generate the corresponding image edits.

More specifically, for the input model sheet m composed of 4 key frames, the forward pass of the SD-XL model adds noise to the encoded latent variable $z = \mathcal{E}(x)$ and produces the noisy variable z_t . We learn a network ϵ_θ to predict the noise added to the diffused latents z_t , conditioned with the edited by Prompt-to-Prompt [19] model sheet c_M and the text prompt c_T , by optimizing the conditioned latent diffu-

243
244
245
246
247
248
249
250
251
252
253
254
255
256
257
258
259
260
261
262
263
264
265
266
267
268
269
270
271
272
273
274

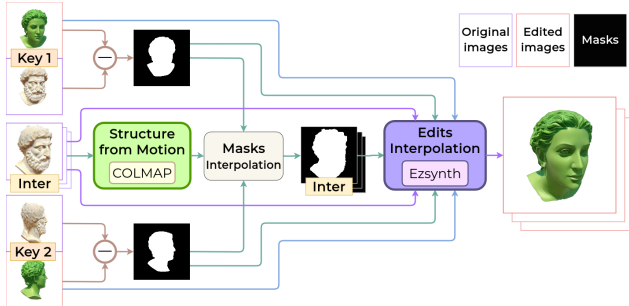
275 sion loss function:

$$276 \quad L = \mathbb{E}_{\mathcal{E}(m), \mathcal{E}(c_M), c_T, \epsilon, t} \left[\|\epsilon - \epsilon_\theta(z_t, t, \mathcal{E}(c_M), c_T)\|_2^2 \right]. \quad (2)$$

277 While the generation process ensures consistency within
278 a single model sheet, it does not guarantee coherence across
279 multiple sheets when edited in separate inference passes.
280 If two model sheets were edited independently, the resulting
281 modifications could diverge, leading to inconsistencies
282 across frames. To maintain uniformity across all original
283 input frames, we propose interpolating the edited outputs of
284 a single model sheet rather than generating new sheets for
285 each edit. This approach prevents discrepancies between
286 successive generations and ensures a more temporally and
287 structurally consistent editing process.

288 4.3. Interpolation

289 Since MV Instruct Pix2Pix XL generates edits for only a
290 subset of frames from the model sheet, it is necessary to
291 propagate these modifications to the remaining input images.
292 To achieve this, we interpolate the content of the
293 edited model sheet frames into the corresponding unmodified
294 poses, effectively transferring the new edits to the entire
295 sequence. The interpolation process between two key
296 frames is illustrated in Fig. 6.



331 Figure 6. Interpolation process of a single intermediate frame
332 batch given two key frames. Firstly, we classically interpolate only
333 the binary mask of the area to apply edits with some margin, and
334 then the Ezsynth [53] model is used to generate the edited images,
335 given the updated content from the key frames.

336 For this interpolation, we employ the Ezsynth video stylization
337 model [53], which is based on the Recurrent All-
338

339 Pairs Field Transforms (RAFT) model for optical flow [52].
340 In our pipeline, we treat Ezsynth as a black-box component,
341 fine-tuning its hyperparameters to reduce reliance on edge
342 detection, thereby allowing for more significant geometric
343 transformations in the inputs.

344 To ensure high-fidelity interpolation, we constrain the
345 model to modify only the regions that were edited by MV
346 Instruct Pix2Pix XL. For each input frame, we generate a
347 binary mask highlighting the areas requiring interpolation.
348 This is accomplished by first identifying the modified
349 regions in the model sheet frames by computing the differ-
350 ence between the original and edited images and threshold-
351 ing the result to create four binary masks. To refine these
352 masks, we apply morphological opening followed by clos-
353 ing operations.

354 Additionally, since our pipeline incorporates a Struc-
355 ture from Motion (SfM) step for geometry estimation (see
356 Sec. 4.5), we leverage the matched keypoints and estimated
357 homography between sequential frames. This allows us to
358 warp and transform the masks derived from edited model
359 sheets, generating corresponding masks for the remaining
360 frames. These refined masks are then used as input to the
361 interpolation model, enabling it to synthesize realistic and
362 spatially consistent modifications. This approach produces
363 more coherent and visually accurate interpolated frames
364 than directly transforming the edited regions.

365 More specifically, having the key frames $k'_1 = \epsilon_\theta(k_1)$
366 and $k'_2 = \epsilon_\theta(k_2)$ edited with the MV Instruct Pix2Pix XL
367 model ϵ_θ , we can describe the interpolating process as an
368 inference of the learned model ϵ_ψ used to edit the original
369 intermediate frame i into edited frame i' :

$$370 \quad i' = \epsilon_\psi(i, m_i, k'_1, k_1 - k'_1, k'_2, k_2 - k'_2), \quad (3)$$

371 where the m_i mask of the interpolated image i is obtained
372 via computing the homography matrix H between key and
373 inter frames: $m_i = H^{-1}i$.

374 The key contribution of this component is that it ensures
375 consistency between intermediate frames and the already
376 edited key frames generated by MV Instruct Pix2Pix XL.
377 As a result, the final output maintains a unified and seamless
378 sequence, preserving both geometric and visual coherence
379 throughout the edited frames.



380 Figure 5. 2D editing comparison on a simple model sheet of 2 images (a) with original Instruct Pix2Pix (b) and our MV model (c).

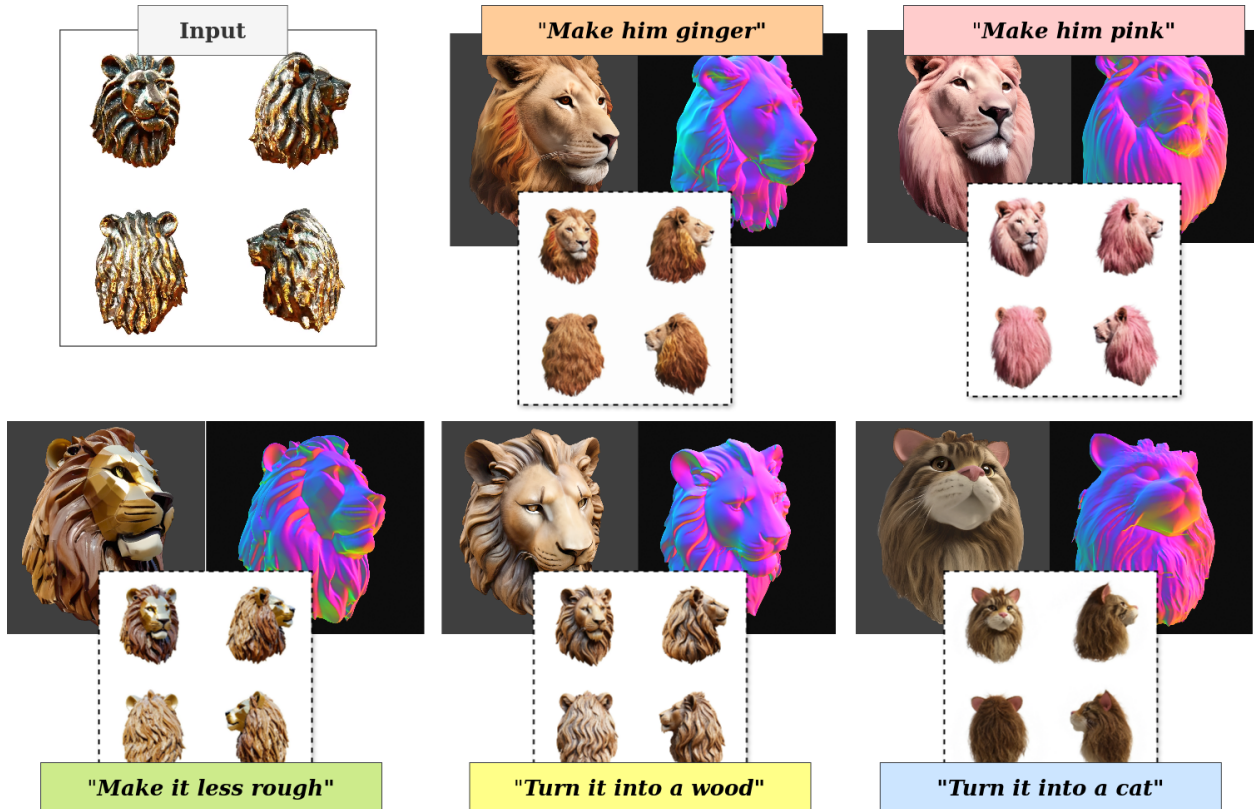


Figure 7. Results of edits with 3D-Pix. The input sequence of a lion is being edited to new 3D models with respect to the input prompts. Our model is capable of producing complex geometry changes (bottom row with structure changes) and appearance changes (top row with color changes).

340

4.4. Super-Resolution

341
342
343
344
345

To further enhance the visual fidelity and detail of the images, we integrate an additional Super-Resolution upscaling model, processing frames in batches of four. For this purpose, we employ the transformer-based Swin2SR model [10].

346

4.5. Structure from Motion

347
348
349
350
351

Since 3D Gaussian Splatting (3D GS) requires an initial sparse point cloud, and our interpolation pipeline (see Sec. 4.3) relies on estimated homographies between frames, we utilize a classical Structure from Motion (SfM) approach from the COLMAP library [40].

352
353
354
355
356
357
358
359
360
361

The SfM reconstruction process is applied exclusively to the original, non-edited images. Running SfM on the edited images often leads to failures due to minor inconsistencies introduced during the editing process, as the traditional COLMAP pipeline lacks robustness against such artifacts. However, performing SfM on the original images consistently succeeds, providing a reliable foundation for subsequent 3D GS optimization with an initial coarse set of features.

4.6. 3D Gaussian Splatting

For the final 3D reconstruction, we employ the original implementation of 3D Gaussian Splatting [22] as a black-box model. The optimization process refines the initial Gaussians obtained from the sparse point cloud to align with the updated, edited appearance. Additionally, we disable the model’s ability to represent view-dependent colors via spherical harmonics (SH) coefficient optimization to maintain consistency in color representation.

5. Experiments

5.1. Instruct Pix2Pix vs Ours

We evaluate the performance of our MV Instruct Pix2Pixel XL model against the original Instruct Pix2Pixel in a 2D editing task using a model sheet. A visual comparison is presented in Fig. 5, demonstrating that our proposed approach achieves greater consistency across different frames. In contrast, the original Instruct Pix2Pixel struggles to maintain high-quality and consistent modifications, even in a simple case of two sequential images.

To quantitatively assess the differences, we compute av-

361

362
363
364
365
366
367
368
369

370

371
372
373
374
375
376
377
378
379
380



Figure 8. Comparison of our 3D-Pix and other open-source models: GaussianEditor [15] and GaussCtrl [59]. While our model performs more robust color changes, other models perform scene-level edits, while we focus only on object-level reconstruction.

381 erage CLIP scores on our dataset and report the results in
 382 Tab. 1. The evaluation considers two key metrics: (1) Similar-
 383 ity to the input image, ensuring that the edited image re-
 384 mains structurally consistent with the original, and (2) Text-
 385 image alignment, measuring the adherence of the edited im-
 386 age to the input textual prompt.

387 For Instruct Pix2Pix, we test two scenarios: processing
 388 a model sheet (similar to our method) and editing individ-
 389 ual frames sequentially (which aligns more closely with the
 390 original model’s training distribution). Our method outper-
 391 forms both cases in terms of text-image alignment, indicat-
 392 ing that it generates more robust and realistic edits. How-
 393 ever, our approach yields lower similarity scores to the input
 394 images, suggesting that it introduces more substantial mod-
 395 ifications compared to the original Instruct Pix2Pix.

396 5.2. Results

397 We present a diverse set of edited 3D assets generated with
 398 3D-Pix in Figs. 1, 2, 5, 7 and 9. Our approach demon-
 399 strates the ability to produce high-quality 3D edits that ac-
 400 curately reflect the desired modifications specified by the
 401 text prompt.

402 We compare our 3D-Pix model with other works in 3D
 403 editing with open source code: GaussianEditor [15] and
 404 GaussCtrl [59] in the Fig. 8. While our solution provides
 405 more robust edits, we perform strictly object-level edits, as
 406 opposed to other models capable of generalizable scene-
 407 level reconstructions.

Instruct Pix2Pix model	CLIP ₁ ↑	CLIP ₂ ↑
Our (model sheet)	0.86	0.14
Original (model sheet)	0.79	0.09
Original (frame-wise)	0.91	0.13

CLIP₁ : Input image similarity

CLIP₂ : Edited text - edited image similarity

Table 1. Comparison of CLIP text and image alignment scores on edited model sheets with our MV Instruct Pix2Pix XL and the original model [4].

408 Our method is effective for both geometric transforma-
 409 tions (e.g., converting an object into a different form) and
 410 appearance modifications (e.g., style or color adjustments).
 411 The generated assets exhibit high fidelity and successfully
 412 capture complex geometric structures while maintaining
 413 consistency across multiple views.

414 5.3. Real-Life Inputs

415 To further evaluate our model’s performance, we apply 3D-
 416 Pix to turntable-style images captured from real-world ob-
 417 jects, as shown in Fig. 9. However, the results indicate a
 418 performance degradation compared to digital input data.

419 Upon analysis of the intermediate outputs, we identify
 420 the primary cause as suboptimal key frame selection, re-
 421 sulting from instability in video recordings, abrupt camera
 422 movements, or sudden shifts in the object’s position. To en-
 423 hance robustness against such real-world artifacts, we pro-
 424 pose integrating a more advanced key frame selection al-
 425 gorithm and applying frame deblurring techniques in future
 426 work to improve editing quality.

427 5.4. Failed Cases

428 Despite its improvements, our approach inherits certain fail-
 429 ure cases from the original Instruct Pix2Pix [4], as illus-
 430 trated in Fig. 10. In some instances, the model fails to iso-
 431 late the specified object components accurately. For exam-
 432 ple, in the ice cream scenario, the model erroneously modi-
 433 fies the green jam instead of the intended waffle. Similarly,
 434 in the goblet case, it struggles to preserve the fine structure
 435 of the input skeleton, resulting in inconsistencies in bone
 436 articulation and subsequent reconstruction artifacts.

437 Furthermore, our 2D editing and interpolation pipeline
 438 occasionally misidentifies elements of an object. For ex-
 439 ample, the top of a glass is misclassified, leading to a non-
 440 transparent blue coloration. Additionally, the model fails to
 441 correctly interpret the internal composition of a goblet, mis-
 442 takenly placing a cherry at its center rather than modifying
 443 its interior as intended.

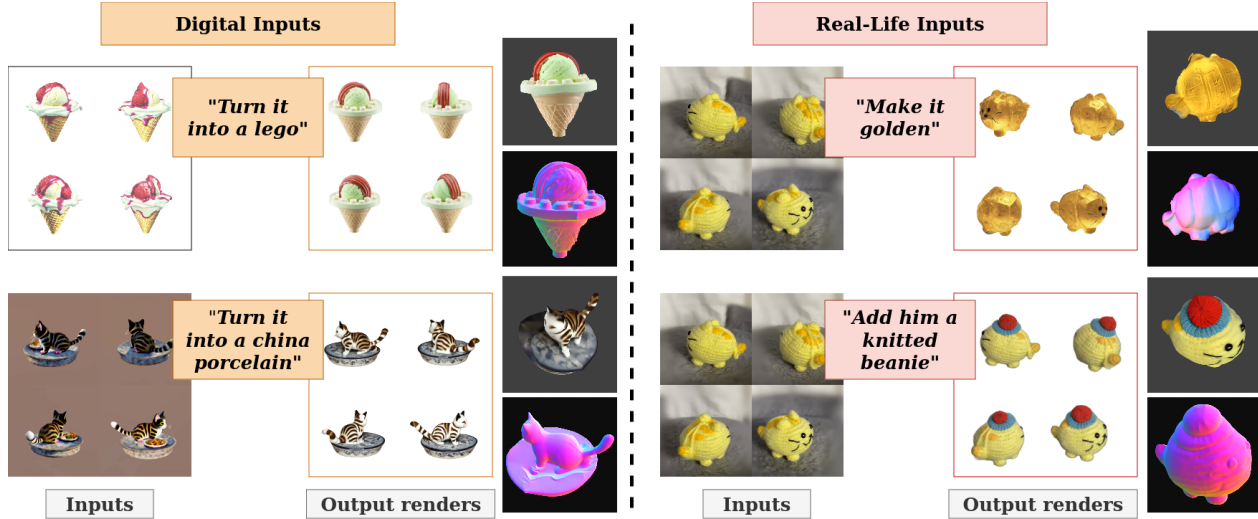


Figure 9. Our 3D-Pix generalizes to both digital (left column) and real-life (right column) inputs.

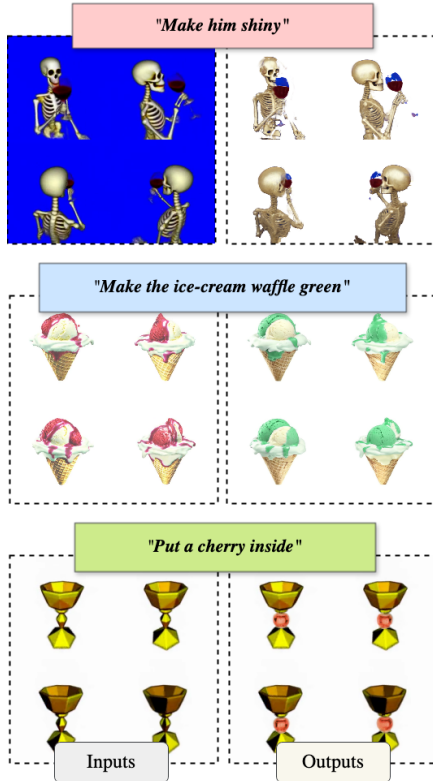


Figure 10. Failed cases. 3D-Pix sometimes struggles with isolating a correct area of the edits (middle and bottom row) or struggles in the thin edges and semi-transparent objects as in the top row.

444

6. Conclusions

445
446
In this work, we introduce MV Instruct Pix2Pix XL, an enhanced version of the Instruct Pix2Pix [4] diffusion model,

adapted for multi-view image editing. Our approach leverages the state-of-the-art (SOTA) SD-XL [37] generative model, extending its capabilities to ensure consistent modifications across multiple viewpoints.

We further demonstrate how MV Instruct Pix2Pix XL enables 3D editing within our 3D-Pix pipeline, a novel framework designed for efficient multi-view object modification. Unlike conventional methods that require multiple inference passes, our approach performs a single inference step, followed by a complex interpolation process to propagate edits across all views while maintaining consistency.

To enhance the visual fidelity of the outputs, we incorporate the Swin2SR [10] super-resolution model for fine-grained image refinement. Additionally, for geometry estimation, we integrate a Structure from Motion (SfM) pipeline, followed by 3D Gaussian Splatting [22], enabling high-quality 3D reconstruction of the edited asset.

Our method is generalizable to both digital and real-world inputs and can serve as a post-hoc refinement stage for any existing 3D generative model, regardless of its underlying geometry representation.

Beyond the scope of 3D editing, our work raises broader questions about adapting 2D generative models to multi-view settings in a structured and scalable manner. We introduce a novel frame interpolation technique, ensuring that modifications applied to a subset of frames are seamlessly propagated, preserving object consistency across multiple perspectives.

This research paves the way for future explorations in multi-view generative modeling, extending beyond editing to tasks such as multi-view synthesis, reconstruction, and consistency-aware generation.

447
448
449
450451
452
453
454
455
456
457458
459
460
461
462
463464
465
466
467468
469
470
471
472
473
474475
476
477
478

479

References

[1] Mohammadreza Armandpour, Ali Sadeghian, Huangjie Zheng, Amir Sadeghian, and Mingyuan Zhou. Re-imagine the negative prompt algorithm: Transform 2d diffusion into 3d, alleviate janus problem and beyond, 2023. 1, 3

[2] Jonathan T. Barron, Ben Mildenhall, Dor Verbin, Pratul P. Srinivasan, and Peter Hedman. Mip-nerf 360: Unbounded anti-aliased neural radiance fields, 2022. 2

[3] Anna-Alina Bondarets, Taras Rumezhak, Hlib Plakhtii, Alina Muliak, and Volodymyr Karpiv. 3d-GSR: 3d super-resolution with multi-view adapter and gaussian splatting. In *ECCV 2024 Workshop on Wild 3D: 3D Modeling, Reconstruction, and Generation in the Wild*, 2024. 3

[4] Tim Brooks, Aleksander Holynski, and Alexei A. Efros. Instructpix2pix: Learning to follow image editing instructions, 2023. 1, 2, 3, 4, 5, 7, 8

[5] Tom B. Brown, Benjamin Mann, Nick Ryder, Melanie Subbiah, Jared Kaplan, Prafulla Dhariwal, Arvind Neelakantan, Pranav Shyam, Girish Sastry, Amanda Askell, Sandhini Agarwal, Ariel Herbert-Voss, Gretchen Krueger, Tom Henighan, Rewon Child, Aditya Ramesh, Daniel M. Ziegler, Jeffrey Wu, Clemens Winter, Christopher Hesse, Mark Chen, Eric Sigler, Mateusz Litwin, Scott Gray, Benjamin Chess, Jack Clark, Christopher Berner, Sam McCandlish, Alec Radford, Ilya Sutskever, and Dario Amodei. Language models are few-shot learners, 2020. 3, 4

[6] Anpei Chen, Zexiang Xu, Fuqiang Zhao, Xiaoshuai Zhang, Fanbo Xiang, Jingyi Yu, and Hao Su. Mvsnerf: Fast generalizable radiance field reconstruction from multi-view stereo, 2021. 2

[7] Zhiqin Chen and Hao Zhang. Learning implicit fields for generative shape modeling, 2019. 2

[8] Zilong Chen, Feng Wang, Yikai Wang, and Huaping Liu. Text-to-3d using gaussian splatting, 2024. 1, 2

[9] Christopher B. Choy, Danfei Xu, JunYoung Gwak, Kevin Chen, and Silvio Savarese. 3d-r2n2: A unified approach for single and multi-view 3d object reconstruction, 2016. 2

[10] Marcos V. Conde, Ui-Jin Choi, Maxime Burchi, and Radu Timofte. Swin2sr: Swinv2 transformer for compressed image super-resolution and restoration, 2022. 6, 8

[11] Matt Deitke, Dustin Schwenk, Jordi Salvador, Luca Weihs, Oscar Michel, Eli VanderBilt, Ludwig Schmidt, Kiana Ehsani, Aniruddha Kembhavi, and Ali Farhadi. Objaverse: A universe of annotated 3d objects, 2022. 4

[12] Congyue Deng, Chiyu "Max" Jiang, Charles R. Qi, Xinchen Yan, Yin Zhou, Leonidas Guibas, and Dragomir Anguelov. Nerd: Single-view nerf synthesis with language-guided diffusion as general image priors, 2022. 1, 3

[13] Kangle Deng, Andrew Liu, Jun-Yan Zhu, and Deva Ramanan. Depth-supervised nerf: Fewer views and faster training for free, 2022. 2

[14] Prafulla Dhariwal and Alex Nichol. Diffusion models beat gans on image synthesis, 2021. 2

[15] Jiemin Fang, Junjie Wang, Xiaopeng Zhang, Lingxi Xie, and Qi Tian. Gaussianeditor: Editing 3d gaussians delicately with text instructions, 2023. 1, 3, 7

[16] Jun Gao, Tianchang Shen, Zian Wang, Wenzheng Chen, Kangxue Yin, Daiqing Li, Or Litany, Zan Gojcic, and Sanja Fidler. Get3d: A generative model of high quality 3d textured shapes learned from images, 2022. 2

[17] Lin Gao, Tong Wu, Yu-Jie Yuan, Ming-Xian Lin, Yu-Kun Lai, and Hao Zhang. Tm-net: Deep generative networks for textured meshes, 2021. 2

[18] Ayaan Haque, Matthew Tancik, Alexei A. Efros, Aleksander Holynski, and Angjoo Kanazawa. Instruct-nerf2nerf: Editing 3d scenes with instructions, 2023. 1, 3

[19] Amir Hertz, Ron Mokady, Jay Tenenbaum, Kfir Aberman, Yael Pritch, and Daniel Cohen-Or. Prompt-to-prompt image editing with cross attention control, 2022. 3, 4

[20] Jonathan Ho, Ajay Jain, and Pieter Abbeel. Denoising diffusion probabilistic models, 2020. 2

[21] Oren Katzir, Or Patashnik, Daniel Cohen-Or, and Dani Lischinski. Noise-free score distillation, 2023. 2

[22] Bernhard Kerbl, Georgios Kopanas, Thomas Leimkühler, and George Drettakis. 3d gaussian splatting for real-time radiance field rendering. *ACM Transactions on Graphics*, 42(4), 2023. 1, 2, 6, 8

[23] Yushi Lan, Feitong Tan, Di Qiu, Qiangeng Xu, Kyle Genova, Zeng Huang, Sean Fanello, Rohit Pandey, Thomas Funkhouser, Chen Change Loy, and Yinda Zhang. Gaussian3diff: 3d gaussian diffusion for 3d full head synthesis and editing. In *ECCV*, 2024. 2

[24] Xinhai Li, Huaibin Wang, and Kuo-Kun Tseng. Gaussiandiffusion: 3d gaussian splatting for denoising diffusion probabilistic models with structured noise, 2023. 2

[25] Ivan Lopes, Fabio Pizzati, and Raoul de Charette. Material palette: Extraction of materials from a single image, 2023. 3

[26] Shitong Luo and Wei Hu. Diffusion probabilistic models for 3d point cloud generation, 2021. 2

[27] Luke Melas-Kyriazi, Christian Rupprecht, Iro Laina, and Andrea Vedaldi. Realfusion: 360deg reconstruction of any object from a single image, 2023. 1, 3

[28] Lars Mescheder, Michael Oechsle, Michael Niemeyer, Sebastian Nowozin, and Andreas Geiger. Occupancy networks: Learning 3d reconstruction in function space, 2019. 2

[29] Gal Metzer, Elad Richardson, Or Patashnik, Raja Giryes, and Daniel Cohen-Or. Latent-nerf for shape-guided generation of 3d shapes and textures, 2022. 1, 2, 3

[30] Ben Mildenhall, Pratul P. Srinivasan, Matthew Tancik, Jonathan T. Barron, Ravi Ramamoorthi, and Ren Ng. Nerf: Representing scenes as neural radiance fields for view synthesis, 2020. 2

[31] Yuxuan Mu, Xinxin Zuo, Chuan Guo, Yilin Wang, Juwei Lu, Xiaofeng Wu, Songcen Xu, Peng Dai, Youliang Yan, and Li Cheng. Gsd: View-guided gaussian splatting diffusion for 3d reconstruction, 2024. 2

[32] Alex Nichol, Heewoo Jun, Prafulla Dhariwal, Pamela Mishkin, and Mark Chen. Point-e: A system for generating 3d point clouds from complex prompts, 2022. 1, 2

[33] Beatrix M. G. Nielsen, Anders Christensen, Andrea Dittadi, and Ole Winther. Diffenc: Variational diffusion with a learned encoder, 2024. 2

591 [34] Francesco Palandra, Andrea Sanchietti, Daniele Baieri, and
592 Emanuele Rodolà. Gsedit: Efficient text-guided editing of
593 3d objects via gaussian splatting, 2024. 1, 3

594 [35] Gaurav Parmar, Krishna Kumar Singh, Richard Zhang, Yijun
595 Li, Jingwan Lu, and Jun-Yan Zhu. Zero-shot image-to-image
596 translation, 2023. 1, 3

597 [36] Dario Pavllo, Jonas Kohler, Thomas Hofmann, and Aurelien
598 Lucchi. Learning generative models of textured 3d meshes
599 from real-world images, 2021. 2

600 [37] Dustin Podell, Zion English, Kyle Lacey, Andreas
601 Blattmann, Tim Dockhorn, Jonas Müller, Joe Penna, and
602 Robin Rombach. Sdxl: Improving latent diffusion models
603 for high-resolution image synthesis, 2023. 1, 2, 4, 8

604 [38] Ben Poole, Ajay Jain, Jonathan T. Barron, and Ben Mildenhall.
605 Dreamfusion: Text-to-3d using 2d diffusion, 2022. 1,
606 2

607 [39] Robin Rombach, Andreas Blattmann, Dominik Lorenz,
608 Patrick Esser, and Björn Ommer. High-resolution image syn-
609 thesis with latent diffusion models, 2021. 2, 3, 4

610 [40] Johannes Lutz Schönberger and Jan-Michael Frahm.
611 Structure-from-motion revisited. In *Conference on Com-
612 puter Vision and Pattern Recognition (CVPR)*, 2016. 6

613 [41] Katja Schwarz, Axel Sauer, Michael Niemeyer, Yiyi Liao,
614 and Andreas Geiger. Voxgraf: Fast 3d-aware image synthesis
615 with sparse voxel grids, 2022. 2

616 [42] Tianchang Shen, Jun Gao, Kangxue Yin, Ming-Yu Liu, and
617 Sanja Fidler. Deep marching tetrahedra: a hybrid represen-
618 tation for high-resolution 3d shape synthesis, 2021. 2

619 [43] Yichun Shi, Peng Wang, Jianglong Ye, Mai Long, Kejie Li,
620 and Xiao Yang. Mvdream: Multi-view diffusion for 3d gen-
621 eration, 2024. 1, 2, 3, 4

622 [44] Jaehyeok Shim, Changwoo Kang, and Kyungdon Joo.
623 Diffusion-based signed distance fields for 3d shape gener-
624 ation. In *Proceedings of the IEEE/CVF Conference on Com-
625 puter Vision and Pattern Recognition (CVPR)*, pages 20887–
626 20897, 2023. 2

627 [45] Jascha Sohl-Dickstein, Eric A. Weiss, Niru Mah-
628 eswaranathan, and Surya Ganguli. Deep unsupervised
629 learning using nonequilibrium thermodynamics, 2015. 2

630 [46] Jiaming Song, Chenlin Meng, and Stefano Ermon. Denois-
631 ing diffusion implicit models, 2022. 2

632 [47] Jingxiang Sun, Bo Zhang, Ruizhi Shao, Lizhen Wang, Wen
633 Liu, Zhenda Xie, and Yebin Liu. Dreamcraft3d: Hierarchical
634 3d generation with bootstrapped diffusion prior, 2023. 1, 2

635 [48] Yongbin Sun, Yue Wang, Ziwei Liu, Joshua E. Siegel, and
636 Sanjay E. Sarma. Pointgrow: Autoregressively learned point
637 cloud generation with self-attention, 2019. 2

638 [49] Junshu Tang, Tengfei Wang, Bo Zhang, Ting Zhang, Ran Yi,
639 Lizhuang Ma, and Dong Chen. Make-it-3d: High-fidelity 3d
640 creation from a single image with diffusion prior, 2023. 1, 3

641 [50] Jiaxiang Tang, Jiawei Ren, Hang Zhou, Ziwei Liu, and Gang
642 Zeng. Dreamgaussian: Generative gaussian splatting for ef-
643 ficient 3d content creation, 2024. 1, 3

644 [51] Shitao Tang, Fuyang Zhang, Jiacheng Chen, Peng Wang, and
645 Yasutaka Furukawa. Mvdiffusion: Enabling holistic multi-
646 view image generation with correspondence-aware diffusion.
647 *arXiv*, 2023. 2

52] Zachary Teed and Jia Deng. Raft: Recurrent all-pairs field
transforms for optical flow, 2020. 5

53] pravdomil Trentonom0r3. Ezsynth - ebsynth python library,
2023. 5

54] Dor Verbin, Peter Hedman, Ben Mildenhall, Todd Zickler,
Jonathan T. Barron, and Pratul P. Srinivasan. Ref-nerf: Struc-
55 tured view-dependent appearance for neural radiance fields,
2021. 2

55] Guangcong Wang, Zhaoxi Chen, Chen Change Loy, and Zi-
wei Liu. Sparsenerf: Distilling depth ranking for few-shot
56 novel view synthesis, 2023. 2

56] Nanyang Wang, Yinda Zhang, Zhiwen Li, Yanwei Fu, Wei
Liu, and Yu-Gang Jiang. Pixel2mesh: Generating 3d mesh
models from single rgb images, 2018. 2

57] Yuxuan Wang, Xuanyu Yi, Zike Wu, Na Zhao, Long Chen,
and Hanwang Zhang. View-consistent 3d editing with gaus-
58 sian splatting, 2025. 3

59] Zhengyi Wang, Cheng Lu, Yikai Wang, Fan Bao, Chongxuan
Li, Hang Su, and Jun Zhu. Prolificdreamer: High-fidelity and
59 diverse text-to-3d generation with variational score distilla-
60 tion, 2023. 1, 2

61] Jing Wu, Jia-Wang Bian, Xinghui Li, Guangrun Wang, Ian
Reid, Philip Torr, and Victor Adrian Prisacariu. Gaussctrl:
62 Multi-view consistent text-driven 3d gaussian splatting edit-
63 ing, 2024. 3, 7

64] Tim Z. Xiao, Johannes Zenn, and Robert Bamler. Upgrading
65 vae training with unlimited data plans provided by diffusion
66 models, 2023. 2

67] Dejia Xu, Yifan Jiang, Peihao Wang, Zhiwen Fan, Yi Wang,
68 and Zhangyang Wang. Neurallift-360: Lifting an in-the-wild
69 2d photo to a 3d object with 360deg views, 2023. 1, 3

70] Dejia Xu, Ye Yuan, Morteza Mardani, Sifei Liu, Jiaming
Song, Zhangyang Wang, and Arash Vahdat. Agg: Amor-
71 tized generative 3d gaussians for single image to 3d, 2024.
72

73] Guandao Yang, Xun Huang, Zekun Hao, Ming-Yu Liu, Serge
74 Belongie, and Bharath Hariharan. Pointflow: 3d point cloud
75 generation with continuous normalizing flows, 2019. 2

76] Lior Yariv, Omri Puny, Natalia Neverova, Oran Gafni, and
77 Yaron Lipman. Mosaic-sdf for 3d generative models, 2024.
78

79] Taoran Yi, Jiemin Fang, Junjie Wang, Guanjun Wu, Lingxi
80 Xie, Xiaopeng Zhang, Wenyu Liu, Qi Tian, and Xinggang
81 Wang. Gaussiandreamer: Fast generation from text to 3d
82 gaussians by bridging 2d and 3d diffusion models, 2023. 2

83] Kim Youwang, Tae-Hyun Oh, and Gerard Pons-Moll. Paint-
84 it: Text-to-texture synthesis via deep convolutional texture
85 map optimization and physically-based rendering, 2023. 3

86] Alex Yu, Sara Fridovich-Keil, Matthew Tancik, Qinhong
87 Chen, Benjamin Recht, and Angjoo Kanazawa. Plenoxels:
88 Radiance fields without neural networks, 2021. 2

89] Alex Yu, Vickie Ye, Matthew Tancik, and Angjoo Kanazawa.
90 pixelnerf: Neural radiance fields from one or few images,
91 2021. 2

92] Hu Yu, Li Shen, Jie Huang, Man Zhou, Hongsheng Li, and
93 Feng Zhao. Debias the training of diffusion models, 2023. 2

704 [70] Jianhui Yu, Hao Zhu, Liming Jiang, Chen Change Loy, Wei-
705 dong Cai, and Wayne Wu. Painthuman: Towards high-
706 fidelity text-to-3d human texturing via denoised score dis-
707 tillation, 2023. [1](#), [2](#)

708 [71] Xin Yu, Yuan-Chen Guo, Yangguang Li, Ding Liang, Song-
709 Hai Zhang, and Xiaojuan Qi. Text-to-3d with classifier score
710 distillation, 2023. [1](#), [2](#)

711 [72] Bohan Zeng, Shanglin Li, Yutang Feng, Hong Li, Sicheng
712 Gao, Jiaming Liu, Huaxia Li, Xu Tang, Jianzhuang Liu, and
713 Baochang Zhang. Ipdreamer: Appearance-controllable 3d
714 object generation with image prompts, 2024. [1](#), [3](#)

715 [73] Xiaohui Zeng, Arash Vahdat, Francis Williams, Zan Gojcic,
716 Or Litany, Sanja Fidler, and Karsten Kreis. Lion: Latent
717 point diffusion models for 3d shape generation, 2022. [2](#)

718 [74] Biao Zhang, Matthias Nießner, and Peter Wonka. 3dilg: Ir-
719 regular latent grids for 3d generative modeling, 2022. [2](#)

720 [75] Biao Zhang, Jiapeng Tang, Matthias Niessner, and Peter
721 Wonka. 3dshape2vecset: A 3d shape representation for neu-
722 ral fields and generative diffusion models, 2023. [2](#)

723 [76] Lvmin Zhang, Anyi Rao, and Maneesh Agrawala. Adding
724 conditional control to text-to-image diffusion models, 2023.
725 [3](#)

726 [77] Zhenkai Zhang, Krista A. Ehinger, and Tom Drummond. Im-
727 proving denoising diffusion models via simultaneous estima-
728 tion of image and noise, 2023. [2](#)